

Supplementary Material

Table S1. Selected vibration frequencies (in cm^{-1}) of investigated quinoxalines **1a–3c** obtained from FT-IR spectra.

Compd.	$\tilde{\nu}$ (cm^{-1})
1a	3047, 2995, 2966, 1626 (C=O), 1588, 1500, 1466, 1401, 1351, 1252, 1180, 1131, 1116, 1088, 1075, 1036, 953, 850, 837, 827, 797, 741, 706, 471
1b	3048, 2983, 2939, 1620 (C=O), 1574, 1496, 1464, 1405, 1378, 1266, 1237, 1197, 1166, 1138, 1115, 833, 799, 741, 731, 483
1c	3058, 2989, 2927, 1632 (C=O), 1585, 1490, 1460, 1444, 1357, 1248, 1201, 1175, 1157, 1091, 1075, 1023, 825, 806, 776, 742, 701, 588, 467
2a	3056, 2986, 2927, 1724 (C=O, ester), 1623 (C=O), 1590, 1498, 1462, 1411, 1386, 1358, 1309, 1241, 1173, 1121, 1083, 1032, 825, 784, 743, 477
2b	3037, 2981, 2931, 1726, 1695 (C=O, ester), 1623 (C=O), 1592, 1490, 1457, 1376, 1365, 1320, 1294, 1230, 1199, 1175, 1118, 1077, 1030, 846, 822, 787, 714, 678, 481
2c	3058, 2984, 2929, 1726, 1685 (C=O, ester), 1636 (C=O), 1612, 1590, 1534, 1480, 1452, 1365, 1355, 1318, 1245, 1224, 1194, 1126, 1096, 1077, 1018, 802, 782, 765, 703, 697, 474
3a	3435 (OH), 3059, 2983, 2603 (dimer), 1720 (C=O, acid), 1619 (C=O), 1541, 1522, 1465, 1439, 1374, 1352, 1260, 1228, 1188, 1122, 1042, 872, 827, 793, 768, 479
3b	3439 (OH), 3052, 2991, 2614 (dimer), 1733 (C=O, acid), 1621 (C=O), 1556, 1536, 1443, 1375, 1335, 1256, 1234, 1188, 1120, 1091, 1006, 882, 846, 824, 789, 719, 482
3c	3439 (OH), 3039, 2610 (dimer), 1724 (C=O, acid), 1620 (C=O), 1597, 1533, 1513, 1473, 1458, 1445, 1376, 1357, 1315, 1277, 1255, 1227, 1202, 1095, 1027, 805, 783, 768, 699, 606, 480

Figure S1. Plots of the B3LYP(IEFPCM = DMSO) molecular orbitals contributing to the selected optical transitions of quinoxaline derivatives (λ represents the calculated absorption maximum and f its oscillator strength): (a) **1a**; (b) **1c**. The depicted isosurface value is 0.035 a.u.

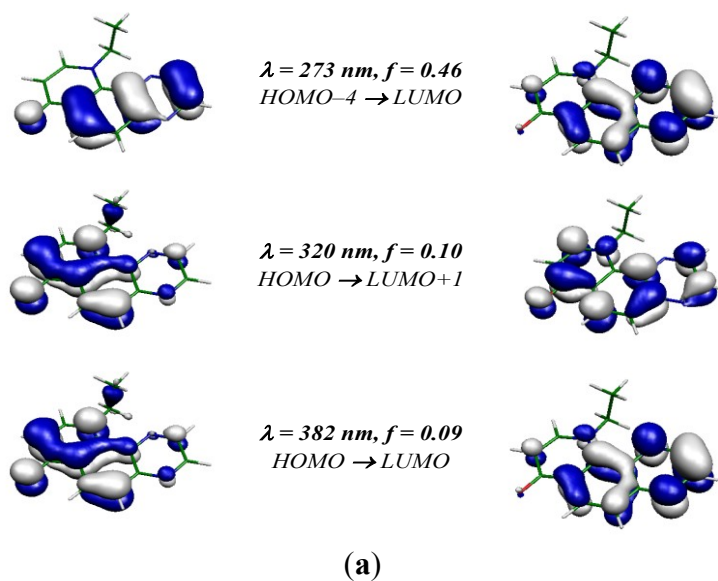


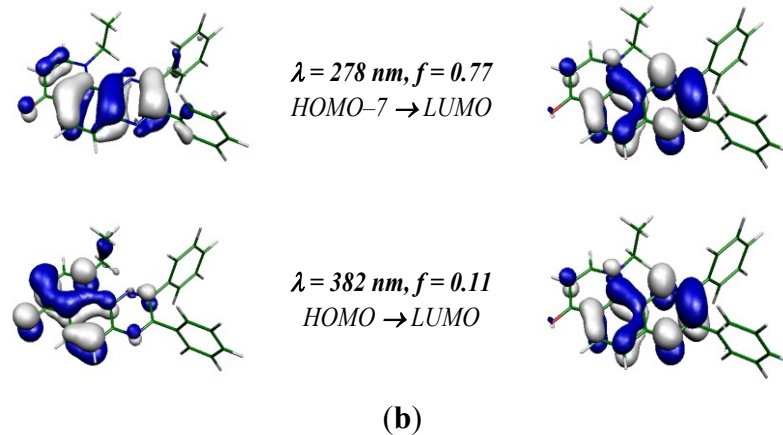
Figure S1. *Cont.*

Figure S2. Experimental (black) and simulated (red) EPR spectra ($SW = 7 \text{ mT}$) obtained upon irradiation ($\lambda_{\max} = 365 \text{ nm}$; irradiance 15 mW cm^{-2}) of the aerated dimethylsulfoxide solutions of (a) **1a**, (b) **3a**, (c) **1c** and (d) **3c** in the presence of DMPO spin trapping agent. Initial concentrations of quinoxalines $c_{0,Q} = 0.8 \text{ mM}$; $c_{0,\text{DMPO}} = 0.02 \text{ M}$. [Solution of **3c** contains equimolar amount of NaOH in DMSO/water (200:1 v:v)]. Simulations represent linear combinations of the corresponding spin-adducts (hfcc parameters listed in Table 2): (a) ${}^{\bullet}\text{DMPO-O}_2^-$ (relative concentration in %; 74), ${}^{\bullet}\text{DMPO-OCH}_3$ (22) and ${}^{\bullet}\text{DMPO-OR}$ (4); (b) ${}^{\bullet}\text{DMPO-O}_2^-$ (51), ${}^{\bullet}\text{DMPO-OCH}_3$ (41), ${}^{\bullet}\text{DMPO-OR}$ (6), ${}^{\bullet}\text{DMPO-CH}_3$ (1.5) and ${}^{\bullet}\text{DMPO}_{\text{degr}}$ (0.5); (c) ${}^{\bullet}\text{DMPO-O}_2^-$ (78), ${}^{\bullet}\text{DMPO-OCH}_3$ (8), ${}^{\bullet}\text{DMPO-OR}$ (7), ${}^{\bullet}\text{DMPO-CH}_3$ (6) and ${}^{\bullet}\text{DMPO}_{\text{degr}}$ (1); (d) ${}^{\bullet}\text{DMPO-O}_2^-$ (62), ${}^{\bullet}\text{DMPO-OCH}_3$ (27) and ${}^{\bullet}\text{DMPO-OR}$ (11).

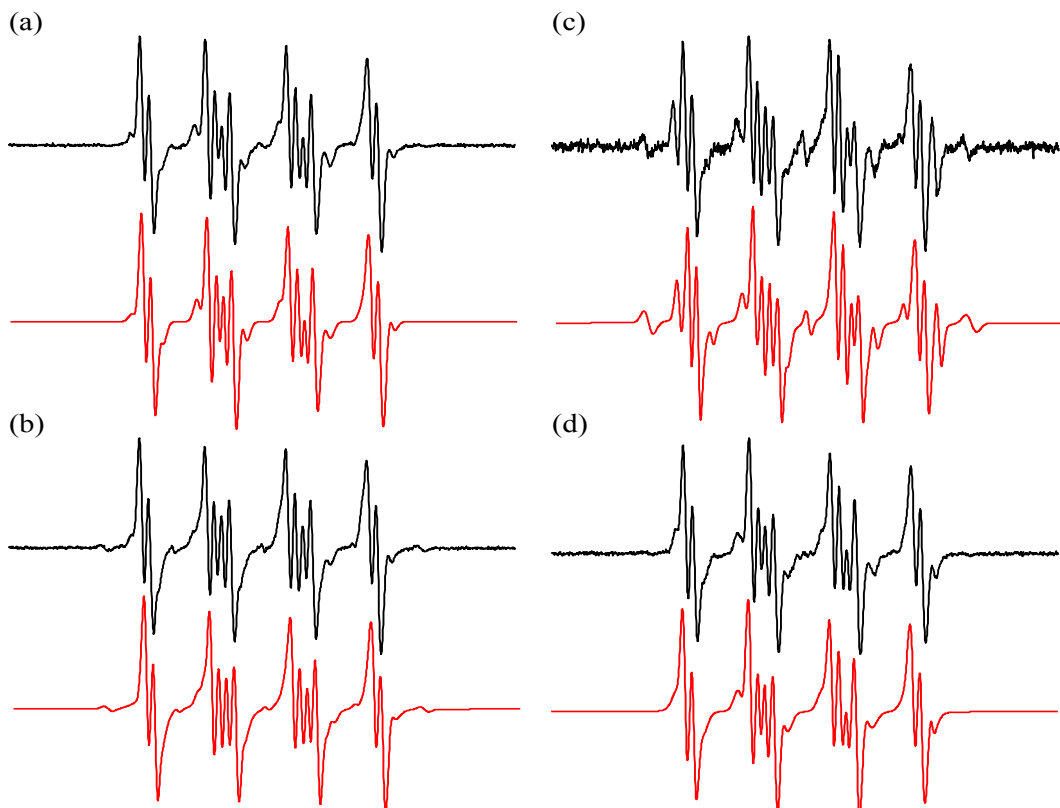


Figure S3. Experimental (black) and simulated (red) EPR spectra ($SW = 8$ mT) obtained upon irradiation ($\lambda_{\max} = 365$ nm; irradiance 15 mW cm^{-2}) of the argon saturated DMSO solutions of (a,b) **3b** and (c,d) **3c** in the presence of (a,c) DMPO or (b,d) ND spin trapping agent. Initial concentrations of quinoxalines $c_{0,Q} = 0.8 \text{ mM}$; $c_{0,\text{DMPO}} = 0.02 \text{ M}$; $c_{0,\text{ND}} \sim 10 \text{ mg mL}^{-1}$. [Solution of **3c** contains equimolar amount of NaOH in DMSO/water (200:1 v:v)]. Simulations represent linear combinations of the corresponding spin-adducts (hfcc parameters listed in Table 2): (a) ${}^{\bullet}\text{DMPO-CH}_3$ (relative concentration in %; 100); (b) ${}^{\bullet}\text{ND-CH}_3$ (88) and ${}^{\bullet}\text{ND-(CH}_2\text{)}_{\text{ar}}$ (12); (c) ${}^{\bullet}\text{DMPO-CH}_3$ (100); (d) ${}^{\bullet}\text{ND-CH}_3$ (83); ${}^{\bullet}\text{ND-CR}_1$ (15) and $\text{ND}^{\bullet-}$ (2; $a_N = 1.378 \text{ mT}$; $g = 2.0061$).

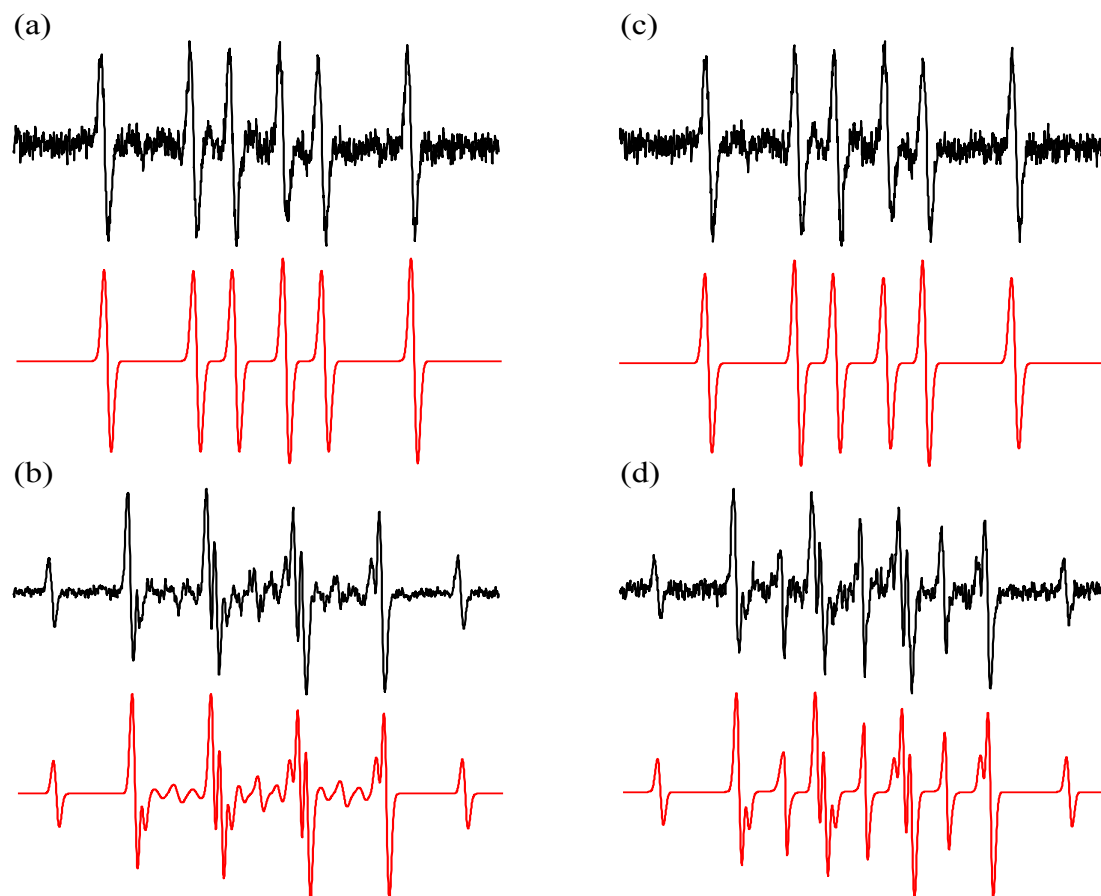


Figure S4. Experimental (black) and simulated (red) EPR spectra ($SW = 7$ mT) obtained after 15 min of irradiation ($\lambda_{\max} = 365$ nm; irradiance 15 mW cm^{-2}) of the aerated solutions of **2b** in mixed solvent DMSO/H₂O (1:1 v:v) containing DMPO or EMPO spin trapping agent with the addition of SOD or sodium azide. **(a)** **2b**/DMPO; **(b)** **2b**/DMPO/SOD; **(c)** **2b**/DMPO/NaN₃; **(d)** **2b**/EMPO, **(e)** **2b**/EMPO/SOD; **(f)** **2b**/EMPO/NaN₃. Initial concentrations of quinoxalines $c_{0,Q} = 0.5$ mM; $c_{0,\text{DMPO}} = 0.04$ M; $c_{0,\text{NaN}_3} = 0.015$ M, $c_{0,\text{SOD}} = 447$ units. Simulations represent linear combinations of the corresponding spin-adducts (hfcc parameters listed in Table 2): **(a)** ${}^{\bullet}\text{DMPO-O}_2^-/\text{OOH}$ (relative concentration in %; 58), ${}^{\bullet}\text{DMPO-OCH}_3$ (18) and ${}^{\bullet}\text{DMPO-OH}$ (19); ${}^{\bullet}\text{DMPO-CH}_3$ (3) and ${}^{\bullet}\text{DMPO}_{\text{degr}}$ (2); **(b)** ${}^{\bullet}\text{DMPO-OH}$ (56) and ${}^{\bullet}\text{DMPO-OCH}_3$ (44); **(c)** ${}^{\bullet}\text{DMPO-OH}$ (34); ${}^{\bullet}\text{DMPO-OCH}_3$ (14) and ${}^{\bullet}\text{DMPO-N}_3$ (52); **(d)** *trans*- ${}^{\bullet}\text{EMPO-O}_2^-/\text{OOH}$ (44), *trans*- ${}^{\bullet}\text{EMPO-OCH}_3$ (13), *trans*- ${}^{\bullet}\text{EMPO-OH}$ (38) and ${}^{\bullet}\text{EMPO-CH}_3$ (5); **(e)** *trans*- ${}^{\bullet}\text{EMPO-O}_2^-/\text{OOH}$ (16), *trans*- ${}^{\bullet}\text{EMPO-OCH}_3$ (14), *trans*- ${}^{\bullet}\text{EMPO-OH}$ (21) and ${}^{\bullet}\text{EMPO-CH}_3$ (49). **(f)** *trans*- ${}^{\bullet}\text{EMPO-OH}$ (49), *trans*- ${}^{\bullet}\text{EMPO-OCH}_3$ (23), ${}^{\bullet}\text{EMPO-N}_3$ (22) and ${}^{\bullet}\text{EMPO-CH}_3$ (6).

